Zirconia-containing radiopaque mesoporous bioactive glasses

Francesca Tallia[a,1], Marta Gallo[b,2], Lucia Pontiroli[a], Francesco Baino[b], Sonia Fiorilli[b], Barbara Onida[b], Giovanni C. Anselmetti[c], Antonio Manca[d], Chiara Vitale-Brovarone[a,b*]

[a] Bionica Tech S.r.l., Corso G. Sommeiller 32, 10128 Torino, Italy

[b] Dipartimento di Scienza Applicata e Tecnologia, Politecnico di Torino, Corso Duca degli Abruzzi 24, 10129 Torino, Italy

[c] GVM-Care & Research - Villapia Hospital, Strada Comunale di Mongreno 180, 10132 Torino, Italy

[d] Radiology Unit , Istituto di Candiolo – IRCCS, Fondazione del Piemonte per l'Oncologia, Strada Provinciale 142 km 3.95, 10060 Candiolo (Torino), Italy

*Corresponding author: Tel: +39 011 5644716; E-mail: chiara.vitale@polito.it

Abstract

A radiopaque mesoporous bioactive glass (named MBGZ-7) was obtained through a combined sol-gel and evaporation induced self-assembling (EISA) route, adding zirconium propoxide to the synthesis batch as the zirconia precursor. The nitrogen sorption analysis confirmed the mesoporous nature of the glass. The assessment of *in vitro* bioactivity by soaking in acellular simulated body fluid (SBF) and SEM observation showed the deposition of hydroxyapatite crystals on its surface after one week. The good radiopacity level was demonstrated by comparing X-Ray images of MBGZ-7 and a blank sample that did not contain radiopaque additives. It is envisaged the use of MBGZ-7 as a promising dispersed phase in composite materials for minimally invasive surgery procedures, such as injectable bone cements, in order to allow the visualization of the implant under fluoroscopic control, during both injection and follow-up.

Keywords

Radiopacity; Mesoporous bioactive glass; Zirconia; Sol-gel preparation; Bone tissue engineering; Injectable cements.

[1] Department of Materials, Imperial College London, South Kensington Campus, Prince Consort Road, SW7 2BP London, United Kingdom

[2] Université de Lyon, INSA-Lyon, Université Lyon 1, MATEIS CNRS UMR 5510, 7 Avenue Jean Capelle, 69621 Villeurbanne Cedex, France

1. Introduction

Radiopacity is an essential feature of bone cements, in order to allow an easy follow-up of the treated patient and, in case of mini-invasive procedures such as vertebroplasty, to allow the injection of the material under fluoroscopic control [1]. Traditionally, the radiopacity of cements is gained through the addition of a radiopaque agent, such as particles of barium sulfate ($BaSO_4$), zirconia (ZrO_2) or iodine-based organic molecules. This particulate dispersed phase has been proven to cause a worsening of the mechanical properties of the cement and to activate macrophages, thereby contributing to bone resorption [2, 3]; in case of release of the iodine-based monomer, a toxic effect on living organisms has also been observed [4, 5].

In order to overcome all these drawbacks, we developed an inherently radiopaque mesoporous bioactive glass meant to be used as a dispersed phase in injectable bone cements, avoiding the use of additional radiopaque particles. The addition of bioactive glass or glass-ceramic particles in bone cements is well known in literature for their ability to bond to the bone tissue [6, 7], as discovered by Hench in 1971 [8, 9]; moreover, the interest on mesoporous bioactive glasses (MBGs) is growing fast because of their reported osteoinductive ability and their drug loading potential [10-13].

Herein, for the first time to the best of the Authors' knowledge, radiopacity is gained through the addition of zirconia (ZrO_2) into a mesoporous glass network, maintaining satisfactory bioactive properties. The production of mesoporous zirconia is widely described in literature [14-16] and, recently, Zhu et al. [17] produced Zr-incorporated MBGs scaffolds using zirconium tetrachloride as the zirconium precursor. We combined the work of Yan et al. [10] on the sol-gel synthesis of MBGs with the work of Liu et al. [15] on mesoporous zirconia in order to produce Zr-containing mesoporous bioactive glasses (named MBGZ-7) using zirconium propoxide as the zirconia precursor. The invention of this novel class of radiopaque mesoporous glasses and their future applications are disclosed in a patent application recently deposited by Vitale-Brovarone et al. [18].

2. Materials and methods

Basing on the sol-gel synthesis described by Yan et al. [10], MBGZ-7 was synthesized by using the commercial non-ionic block copolymer Pluronic P123 ($EO_{20}PO_{70}EO_{20}$, where "EO" is poly(ethylene glycol) and "PO" is poly(propylene glycol)) as an organic surfactant, which acts as structure-directing

agent for pores formation. In a typical synthesis of MBGZ-7 (SiO_2/CaO/P_2O_5/ZrO_2 = 73:15:5:7 molar ratio), a synthesis batch was prepared by dissolving P123 (4.0 g), tetraethyl orthosilicate (TEOS, 6.10 g), calcium nitrate tetrahydrate ($Ca(NO_3)_2 \cdot 4H_2O$, 1.42 g), triethyl phosphate (TEP, 0.73 g), zirconium propoxide (0.92 g), acetylacetone (Acac, which acts as a stabilizer to prevent the zirconium propoxide from uncontrollable hydrolysis and consequent precipitation, 0.10 g [15]) and HCl 0.5 M (1.0 g) in ethanol (60.0 g). All chemicals were purchased from Sigma-Aldrich, Italy, and used as received. This synthesis batch, continuously stirred at 35°C for 24 hours, resulted in a sol that, once casted into Petri dishes, underwent an ageing step (24 h at room temperature followed by 24 h at 120°C), during which the evaporation-induced self-assembly (EISA) process occurred. The dried gel was calcined at 750°C for 5 h in air to obtain the final MBGZ-7 product in form of thin membranes, which were then ground and sieved when needed. For comparison, a traditional mesoporous bioactive glass without zirconia (MBG, SiO_2/CaO/P_2O_5 = 80:15:5 molar ratio) was synthesized by an identical process, avoiding the addition of zirconium propoxide and Acac. Another glass composition (referred to as MBGZ-15), in which the zirconia molar percentage was increased up to 15% to the detriment of the silica content, was also prepared maintaining unchanged the other synthesis and process parameters for purpose of comparison. The obtained powders underwent wide-angle (2θ within 10-70°) X-Ray diffraction (XRD) through a Philips X'Pert diffractometer (Bragg-Brentano camera geometry with Cu Kα incident radiation; working conditions: 40 kV, 30 mA). Long-range order was assessed through low-angle XRD (2θ within 0.6-5°), whereas specific surface area (SSA) and porosity were characterized by N_2 adsorption/desorption measurements at -196°C performed using a Quantachrome Autosorb1. BET SSA was calculated in the relative pressure range 0.04-0.1 and the pore size was evaluated through the BJH method on the isotherm desorption branch.

In vitro bioactivity tests were carried out by soaking MBGZ-7 in simulated body fluid (SBF) [19] at 37°C for 1, 3 and 7 days with refresh of the solution every 48 h to simulate fluid circulation in the human body. After soaking, the samples were dried at room temperature and then investigated through scanning electron microscopy (SEM, FEI Quanta Inspect 200LV) equipped with electron dispersive spectrometer (EDS, EDAX Genesis) for compositional analysis, to monitor the formation of hydroxyapatite (HA) on their surface over time.

X-Ray images of MBG, MBGZ-7 and MBGZ-15 powders were taken with Digital Radiography equipment (Philips PCR Eleva, Philips Medical System DMC GmbH, Hamburg - Germany) with exposure parameters of 45 kV and 100 mA and exposure time of 0.4 s. Plain X-Rays were post-processed with Osirix software for Mac (Pixmeo SARL, Switzerland). A semi-quantitative analysis of radiopacity was performed drawing a round region of interest (ROI) on the center of each sample with a fixed surface area. The program analyzed the radiopacity of the samples obtaining a whole number that was not influenced by the grayscale visualization window. A single plain X-Ray could contain all samples, thus any possible bias due to exposure parameters could not influence the ratio of radiopacity between the different samples.

3. Results

A type IV N_2 sorption isotherm is observed for MBGZ-7 and MBGZ-15 samples, with a hysteresis loop representing the filling of mesopores (Fig. 1). This finding is further supported by low-angle XRD patterns (Supplementary information (SI) – Fig. A), which show a single low-angle XRD peak (2θ = 1.45°, 1.53° and 1.35° for MBG, MBGZ-7 and MBGZ-15, respectively), characteristic of a wormhole structure. A comparison among MBG, MBGZ-7 and MBGZ-15 in terms of specific surface area (SSA), specific volume (Vol), average pore size (d_{BJH}) and XRD basal *d*-spacing (d_{XRD}), calculated through the Bragg law, is reported in Table 1. A broad halo within the range 2θ = 20-30°, typical of amorphous silica, is visible in wide-angle XRD pattern of MBGZ-7 and MBGZ-15 (SI – Fig. B); no signals due to crystalline ZrO_2 phases are observed in any case.

SEM images of MBGZ-7 surface before and after 1 and 7 days of soaking in SBF (Fig. 2a-b-c, respectively) show the progressive nucleation of HA particles, whose composition is confirmed by the EDS spectrum (Fig. 2d). A quantification of Ca/P ratio is not possible because zirconium and phosphorus peaks are overlapped; however, it is clear that, by incrementing the soaking time, the amount of precipitates increases and the structure of HA changes, determining the formation of HA microcrystals after 1 week (Fig. 2c).

From the X-Ray image reported in Fig. 3 it is evident that an increase in zirconia percentage within glass composition determines an enhancement in radiopacity: considering an analogous ROI for all samples (equal to 0.223 cm^2), MBGZ-7 and MBGZ-15 show an increase of 11% and 17% in radiopacity intensity,

respectively, if compared to MBG, whose radiopacity is given only by Ca and P and which therefore cannot be distinguished from bone.

4. Discussion

N_2 sorption isotherms (Fig. 1) and low-angle XRD analyses confirmed that mesoporous bioactive glasses containing zirconia were successfully synthesized. The addition of ZrO_2 (up to 15 mol% with respect to oxides ratio) does not affect the peculiar features of the starting glass structure: both MBGZ-7 and MBGZ-15 show an amorphous microstructure (SI – Fig. B) and maintains an open mesoporous network. As expected for a mesoporous material, the corresponding exposed specific surface area (hundreds of m^2g^{-1}, Table 1) is one order of magnitude higher than the one exhibited by molten glasses (tens of m^2g^{-1} or even less [20]). Consistently with the findings of Zhu et al. [17], MBGZ-7 shows a decrease in SSA if compared to MBG (174 m^2g^{-1} vs. 307 m^2g^{-1}, respectively), ascribed to a lower degree of order of the mesostructure after zirconium addition. However, when a higher ZrO_2 content is introduced (MBGZ-15), an opposite trend is observed, as a SSA increment (262 m^2g^{-1}), with respect to MBGZ-7, is measured. This observation is in contrast with results shown by Zhu et al., which reported a rather large decrease of surface area and pore volume upon the increase of ZrO_2 up to 15 mol%, attributed to the presence of a large amount of crystalline ZrO_2 inside pores after thermal treatment [17]. At variance, MBGZ-15, synthesized herein, maintains a completely amorphous structure, which suggests a high amount of incorporated Zr atoms and their rather uniform distribution throughout the framework. Due to larger size of Zr atoms compared with the other framework elements, an expansion of the mesostructure is retained to occur, affecting the inter-pores distance [21], with an increase of *d* spacing, as evidenced by low-angle XRD pattern, and pores size swelling, as evidenced by N_2 adsorption-desorption isotherm, and a consequent increase of exposed surface area.

A high exposed surface area plays a key role in the bioactive behavior of the resulting material. As already reported by Zhu et al. [17], *in vitro* tests revealed that the presence of ZrO_2 slows the deposition of HA but MBGZ-7 maintains remarkablebioactive properties: indeed, HA particles were easily detected after 1 day of soaking in SBF, becoming a dense layer that completely covered MBGZ-7 surface after 1 week (Fig. 2). Moreover, for the first time, the intrinsic radiopacity of the resulting glass was assessed: MBGZ-7 shows the unique additional value of being inherently radiopaque (Fig. 3), thanks to the introduction of a high atomic number element (Zr) into the network; once the material is implanted, this

feature allows to discriminate MBGZ-7 particles from the surrounding bone under X-Ray control. MBGZ-7 is preferred to MBGZ-15 because, even if they exhibit comparable mesoporous structure and radiopacity, the increase of ZrO_2 content up to 15 mol% can affect the bioactive behavior: zirconia is an intermediate oxide, hence it stabilizes the glass network, reducing its surface reactivity and, consequently, its bioactivity.

Therefore, MBGZ-7 represents a suitable material to be added into composite injectable bone cements, imparting both radiopacity and bioactive properties in only one dispersed phase.

5. Conclusions

A radiopaque mesoporous bioactive glass containing zirconia was successfully developed. It was demonstrated that the addition of zirconium oxide, up to 15 mol%, imparts radiopacity to the glass maintaining a suitable mesoporous structure and a satisfactory bioactive behavior. Therefore, MBGZ-7 particles have the potential to be used as dispersed phase in composite injectable bone cements, which can be visualized under fluoroscopic control during injection and can stimulate *in vivo* bone regeneration.

6. Acknowledgements

The Authors acknowledge a grant for the Lagrange Project - Crt Foundation for Dr. Francesca Tallia.

References

[1] Lewis G. Injectable bone cements for use in vertebroplasty and kyphoplasty: State-of-the-art review. J Biomed Mater Res Part B: Appl Biomater 2006; 76B: 456-68.

[2] Baleani M, Cristofolini L, Minari C, Toni A. Fatigue strength of PMMA bone cement mixed with gentamicin and barium sulphate vs pure PMMA. Proc Inst Mech Eng H: J Engin Med 2003; 217: 9-12.

[3] Lewis G, van Hooy-Corstjens CSJ, Bhattaram A, Koole LH. Influence of the radiopacifier in an acrylic bone cement on its mechanical, thermal, and physical properties: barium sulfate-containing cement versus iodine-containing cement. J Biomed Mater Res Part B: Appl Biomater 2005; 73B: 77-87.

[4] Kjellson F, Brudeli B, McCarthy ID, Lidgren L. Water uptake and release from iodine-containing bone cement. J Biomed Mater Res 2004; 71A: 292-8.

[5] Lewis G. Alternative acrylic bone cement formulations for cemented arthroplasties: present status, key issues, and future prospects. J Biomed Mater Res Part B: Appl Biomater 2008; 84B: 301-19.

[6] Kokubo T, Yoshihara S, Nishimura N, Yamamuro T, Nakamura T. Bioactive bone cement based on $CaO{-}SiO_2{-}P_2O_5$ glass. J Am Ceramic Soc 1991; 74: 1739-41.

[7] Shinzato S, Kobayashi M, Mousa WF, Kamimura M, Neo M, Kitamura Y, et al. Bioactive polymethyl methacrylate-based bone cement: Comparison of glass beads, apatite- and wollastonite-containing glass–ceramic, and hydroxyapatite fillers on mechanical and biological properties. J Biomed Mater Res 2000; 51: 258-72.

[8] Hench LL, Splinter RJ, Allen WC, Greenlee TK. Bonding mechanisms at the interface of ceramic prosthetic materials. J Biomed Mater Res 1971; 5: 117-41.

[9] Kokubo T. Bioactive glass ceramics: properties and applications. Biomaterials 1991; 12: 155-63.

[10] Yan X, Yu C, Zhou X, Tang J, Zhao D. Highly ordered mesoporous bioactive glasses with superior in vitro bone-forming bioactivities. Angew Chem Int Ed 2004; 43: 5980-4.

[11] López-Noriega A, Arcos D, Izquierdo-Barba I, Sakamoto Y, Terasaki O, Vallet-Regí M. Ordered mesoporous bioactive glasses for bone tissue regeneration. Chem Mater 2006; 18: 3137-44.

[12] Zhao L, Yan X, Zhou X, Zhou L, Wang H, Tang J, et al. Mesoporous bioactive glasses for controlled drug release. Micropor Mesopor Mater 2008; 109: 210-5.

[13] Baino F, Fiorilli S, Mortera R, Onida B, Saino E, Visai L, et al. Mesoporous bioactive glass as a multifunctional system for bone regeneration and controlled drug release. J Appl Biomater Function Mater 2012; 10(1): 12-21.

[14] Fang H, Wan T, Shi W, Zhang M. Design and synthesis of large-pore *p6mm* mesoporus zirconia thin films templated by a novel block copolymer. J Non-Cryst Solids 2007; 353: 1657-61.

[15] Liu SG, Wang H, Li JP, Zhao N, Wei W, Sun YH. A facile route to synthesize mesoporous zirconia with ultra high thermal stability. Mater Res Bull 2007; 42: 171-6.

[16] Wu ZG, Zhao YX, Liu DS. The synthesis and characterization of mesoporous silica–zirconia aerogels. Micropor Mesopor Mater 2004; 68: 127-32.

[17] Zhu Y, Zhang Y, Wu C, Fang Y, Yang J, Wang S. The effect of zirconium incorporation on the physiochemical and biological properties of mesoporous bioactive glasses scaffolds. Micropor Mesopor Mater 2011; 143: 311-9.

[18] Vitale-Brovarone C, Verné E, Bergui M, Onida B, Baino F, Miola M, Ferraris S, Tallia F. Injectable osteoinductive bone cements. WO 2011141889 A1.

[19] Kokubo T, Takadama H. How useful is SBF in predicting in vivo bone bioactivity?. Biomaterials 2006; 27: 2907-15.

[20] Sepulveda P, Jones JR, Hench LL. Characterization of melt-derived 45S5 and sol-gel–derived 58S bioactive glasses. J Biomed Mater Res (Appl Biomater) 2001; 58: 734-40.

[21] Soler-Illia GJAA, Crepaldi EL, Grosso D, Sanchez C. Designed synthesis of large-pore mesoporous silica–zirconia thin films with high mixing degree and tunable cubic or 2D-hexagonal mesostructure. J Mater Chem 2004; 14: 1879-86.

Tables

Table 1: Textural parameters of the synthesized glasses obtained from N_2 sorption isotherms

Glass	SSA (m^2g^{-1})	Vol (cm^3g^{-1})	Average d_{BJH} (nm)	d_{XRD} (nm)
MBG	307	185	3.5	6.1
MBGZ-7	174	111	3.3	5.8
MBGZ-15	262	135	3.6	6.5

Figure Captions

Figure 1: Nitrogen sorption isotherms of MBG, MBGZ-7 and MBGZ-15.

Figure 2: SEM and compositional analysis after i*n vitro* bioactivity tests on MBGZ-7: a) surface of the starting glass as such; b) and c) HA deposition after soaking in SBF for 1 day and 1 week respectively; d) EDS spectrum (y-axis in a.u.) of HA agglomerates visible in c). Magnification of reported SEM micrographs are 4000x for 2a), 5000x for 2b) and 6000x for 2c).

Figure 3: X-Ray image that shows the comparison of radiopacity of different glass powders: a) MBG; b) MBGZ-7; c) MBGZ-15.

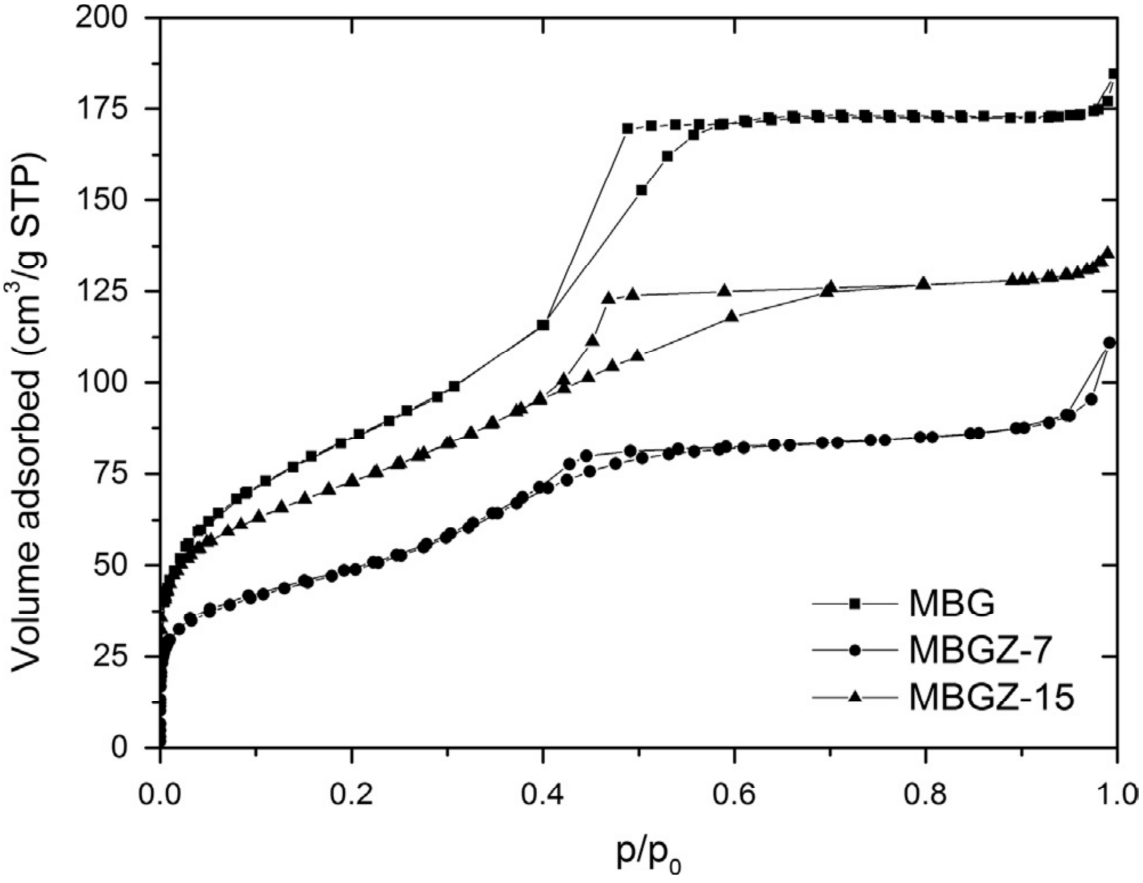
Volume adsorbed (cm3/g STP)
p/p0
MBG
MBGZ-7
MBGZ-15
0
25
50
75
100
125
150
175
200
0.0
0.2
0.4
0.6
0.8
1.0

Fig. 1

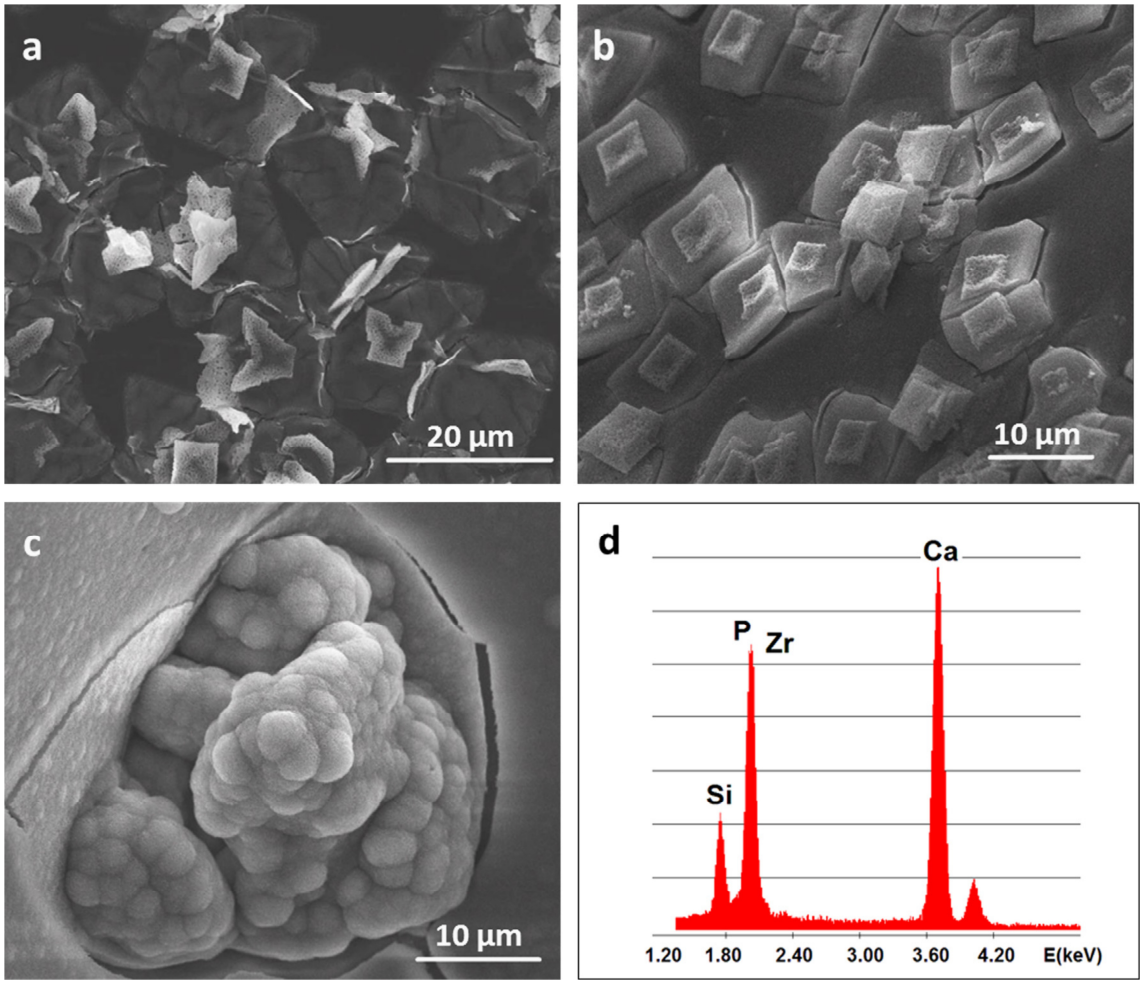

Fig. 2

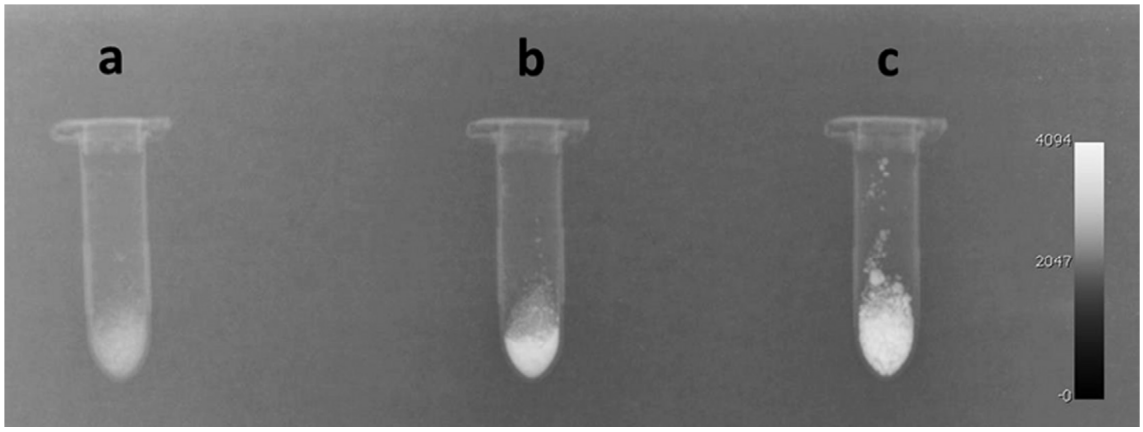

Fig. 3